Geochimica and Cosmochimica Acta

Supporting Information for

Significant impact of hydrothermalism on the biogeochemical signature of sinking and sedimented particles in the Lau Basin

Chloé Tilliette[1], Frédéric Gazeau[1], Valérie Chavagnac[2], Nathalie Leblond[1], Maryline Montanes[1], Karine Leblanc[3], Sabine Schmidt[4], Bruno Charrière[5], Nagib Bhairy[3], Cécile Guieu[1*]

[1]Sorbonne Université, CNRS, Laboratoire d'Océanographie de Villefranche, LOV, 06230, Villefranche-sur-Mer, France
[2]Géosciences Environnement Toulouse, GET, CNRS, UPS, Université de Toulouse, IRD, Toulouse, France
[3]Aix Marseille Univ., Université de Toulon, CNRS, IRD, MIO, Marseille, France.
[4]CNRS, UMR 5805 EPOC, Université de Bordeaux, Pessac, France
[5]Centre de Formation et de Recherche sur l'Environnement Méditerranéen (CEFREM, UMR CNRS 5110), Bât. U, Université de Perpignan, Via Domitia (UPVD), Perpignan, France

Contents of this file

Text S1. Potential biases of sediment traps

Sediment traps have been a standard tool for measuring sinking particle fluxes for decades, yet uncertainties remain regarding their collection efficiency (e.g., Baker et al., 2020; Buesseler et al., 2007; Butman, 1986; Gardner, 1980; Hargrave and Burns, 1979). Advantages of these instruments include their unequivocal separation of sinking material from suspended one, proper preservation of samples for laboratory analyses and accurate sampling periods. Disadvantages include their potential hydrodynamic effects, short collection time-scales (for drifting lines), possible contamination by swimmers and attachment of non-swimming material on them (Buesseler et al., 2007). Such biases could result in under- or over-trapping. Field comparison of different trap designs provided valuable insight into the appropriate procedures for these tools (Baker et al., 2020; Gardner, 1980; Scholten et al., 2001 and references therein). In the present study, efforts were employed to accurately collect sinking particles by **(1)** ensuring that traps were deployed below the mixed layer (Owens et al., 2013), **(2)** focusing the discussion on collected relative weights and elemental ratios rather than material fluxes, and **(3)** unhooking any visible material attached to swimmers whenever possible before removal. Furthermore, the deployment position of the fixed mooring line (i.e., station 12) was predetermined by Ariane modeling simulations (Grima and Maes, pers. comm., 2019) to minimize the impact of regional dynamics features (e.g., current velocities and physical dynamics that can drag the mooring line, tilt the trap or cause upward motions). Although we are aware of these biases, sediment traps remain the only way to collect free-sinking particles from the suspended pool, and fixed traps are the only tool capable of collecting free-sinking material annually in a specific region. The physical conditions of the fixed sediment traps at different deployment depths are described in *Text S2*.

Text S2. Physical conditions of the moored sediment traps

The average depth of the upper and lower sediment traps was 261 ± 16 m (n = 8141) and 1053 ± 15 m (n = 8104), respectively (*Fig. S1a, b*). Rare and short deepening events below 400 and 1190

m occurred in April and June. The average trap pitch angle at 200 m was -2 ± 1° and ranged from -10 to 3°. The trap pitch angle at 1000 m averaged -8 ± 4°, varying between -32 and 1°. It should be noted that high pitch angles (> 10 °) were rather rare, especially for the 200 m-trap (0.02% versus < 30% of the total period for the 1000 m-trap), and mainly associated with trap deepening events and current speeds exceeding 30 cm s^{-1}. The average current velocity at 200 and 1000 m was 10 ± 4 cm s^{-1} and 11 ± 5 cm s^{-1}, respectively. At 200 m, the maximum velocity recorded was 38 cm s^{-1}. At 1000 m, the maximum velocity recorded was 31 cm s^{-1}.

Text S3. Measurements of pH on the total scale

Samples were collected at 11 stations during the TONGA cruise (GPpr14; Guieu and Bonnet, 2019), along a transect extending from New Caledonia to the western end of the South Pacific gyre. At each station, conventional CTD casts were conducted to sample pH and total alkalinity at different depths using a rosette equipped with 24 Niskin bottles (12 L). Samples of 300 mL were collected in glass bottles by completely overflowing the seawater and analyzed within 2 h of collection. The pH on the total scale (pH_T) was measured with an Agilent® Cary60 UV-Vis spectrophotometer. Seawater was transferred to 30 mL quartz cells to measure absorbances at 434 and 578 nm, before and after addition of 50 µL of meta-Cresol purple (Dickson et al., 2007). pH_T was then determined from the absorbance values according to the method described by Liu et al. (2011). The accuracy of pH_T measurements was estimated using a TRIS buffer solution of salinity 35 provided by Andrew Dickson (Scripps Institution of Oceanography, USA). Temperature at the time of measurement was determined using a Traceable® digital thermometer to adjust pH_T to the *in-situ* temperature.

Text S4. Measurements of total alkalinity

Samples of 500 mL were poisoned a few minutes after collection with 100 µL of mercury(II) chloride ($HgCl_2$; 0.02%). Total alkalinity (A_T) was measured using a Metrohm® Titrando 888 titrator and a calibrated Methrom® Ecotrode Plus glass electrode using (1) NBS buffers (pH 4.0 and 7.0 to ensure a Nernstian slope) and then (2) TRIS buffer solution of salinity 35, provided by Andrew Dickson (Scripps Institution of Oceanography, USA). Triplicate titrations were performed on 50 mL subsamples at 25 °C, and A_T was measured as described by Dickson et al. (2007). Titrations of certified material provided by Andrew Dickson (Scripps Institution of Oceanography, USA) returned a A_T value of 2209.374 ± 3.212 µmol kg^{-1} (n = 21), consistent with the nominal value of 2212 µmol kg^{-1} (batch #186).

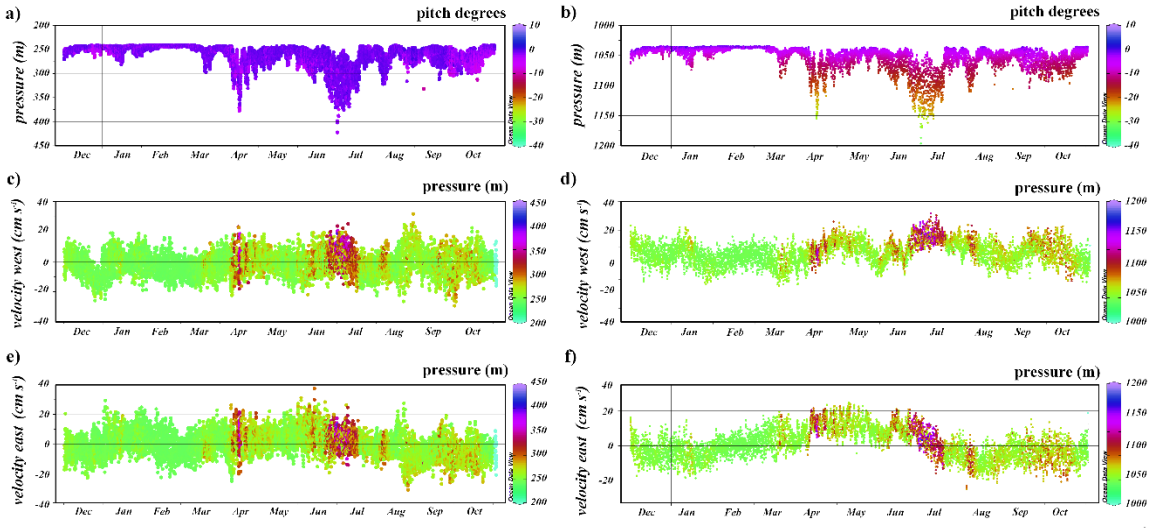

Figure S1. Plots showing inclination angles measured by inclinometers at 222 m **(a)** and 1030 m **(b)** and west and east velocities (cm s^{-1}) measured by current meters at 222 m **(c, e)** and 1030 m **(d, f)** during the fixed mooring line deployment period (from November 2019 to October 2020).

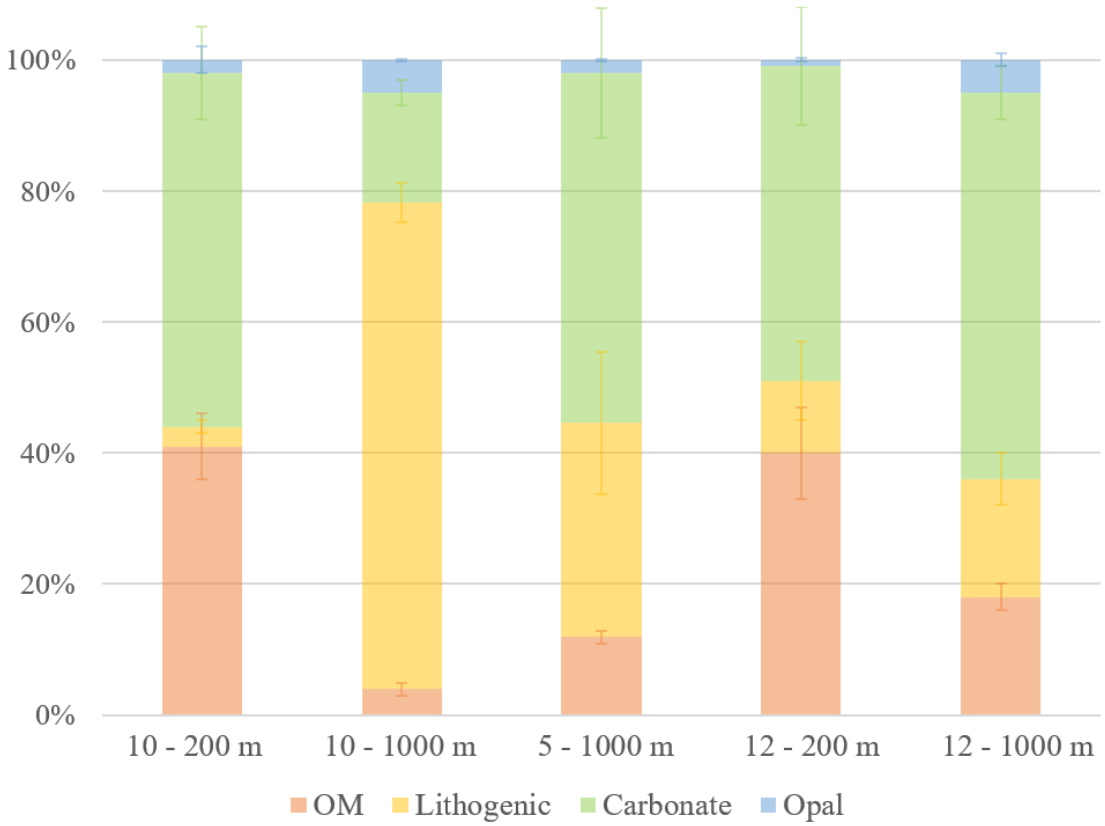

Figure S2. Cumulative histogram of the different fractions of material collected in the sediment traps, averaged over the entire deployment period for drifting traps and over the 2019-2020 austral summer period for fixed traps (i.e., from December 2019 to April 2020). Orange: organic matter, blue: opal, green: calcium carbonate and yellow: lithogenic material.

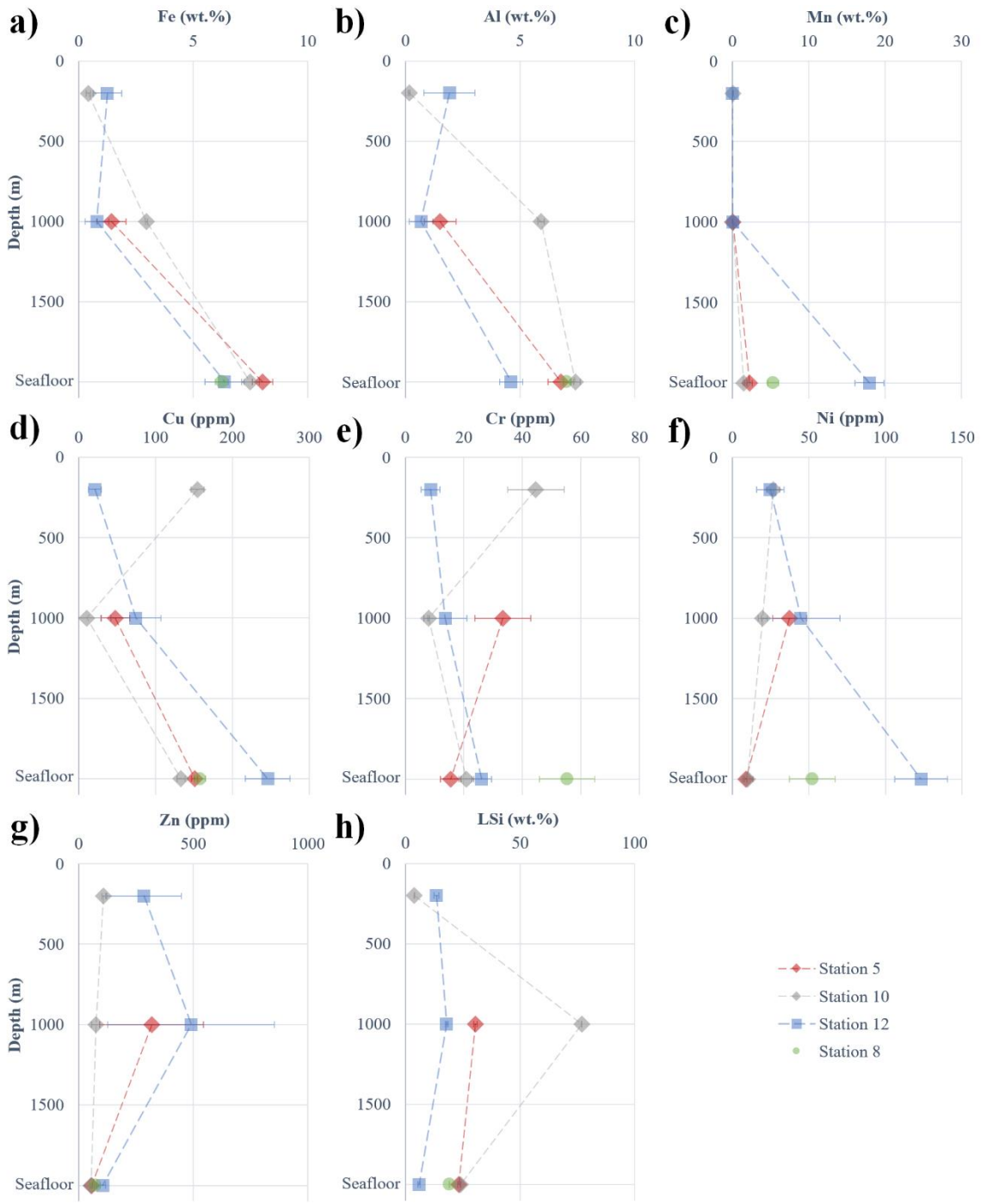

Figure S3. Profiles of particulate **(a)** iron (Fe), **(b)** aluminum (Al), **(c)** manganese (Mn), **(d)** copper (Cu), **(e)** chromium (Cr), **(f)** nickel (Ni), **(g)** zinc (Zn), and **(h)** lithogenic silica (LSi) for the different stations. Fe, Al, Mn and LSi are expressed in wt.% while Cu, Cr, Ni and Zn are expressed in ppm.

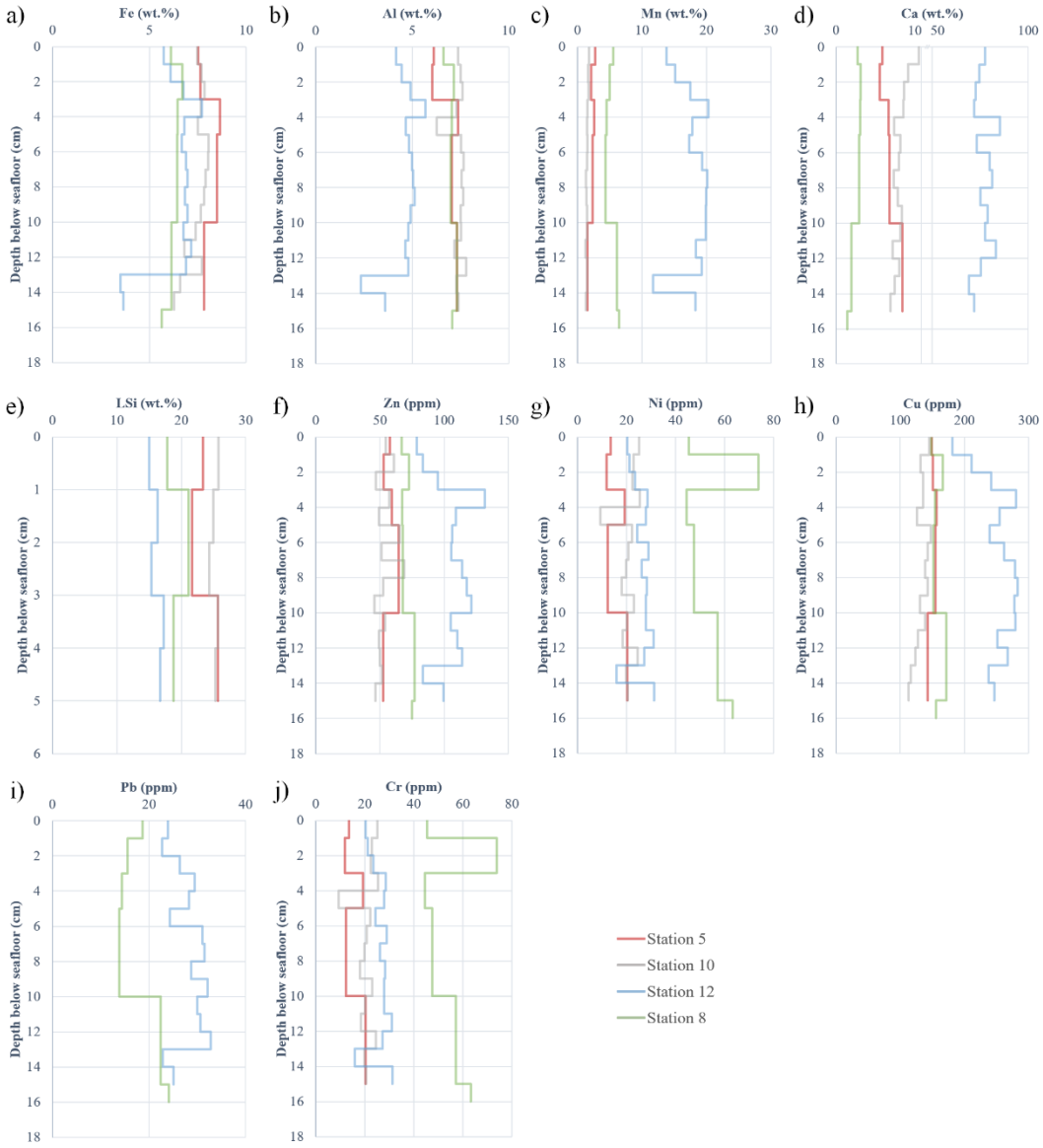

Figure S4. Profiles of particulate **(a)** iron (Fe), **(b)** aluminum (Al), **(c)** manganese (Mn), **(d)** calcium (Ca), **(e)** lithogenic silica (LSi), **(f)** zinc (Zn), **(g)** nickel (Ni), **(h)** copper (Cu), **(i)** lead (Pb) and **(j)** chromium (Cr) from the 15 cm of sediment cored during the cruise. Fe, Al, Mn, Ca and LSi are expressed in wt.% and Zn, Ni, Cu, Pb and Cr are expressed in ppm.

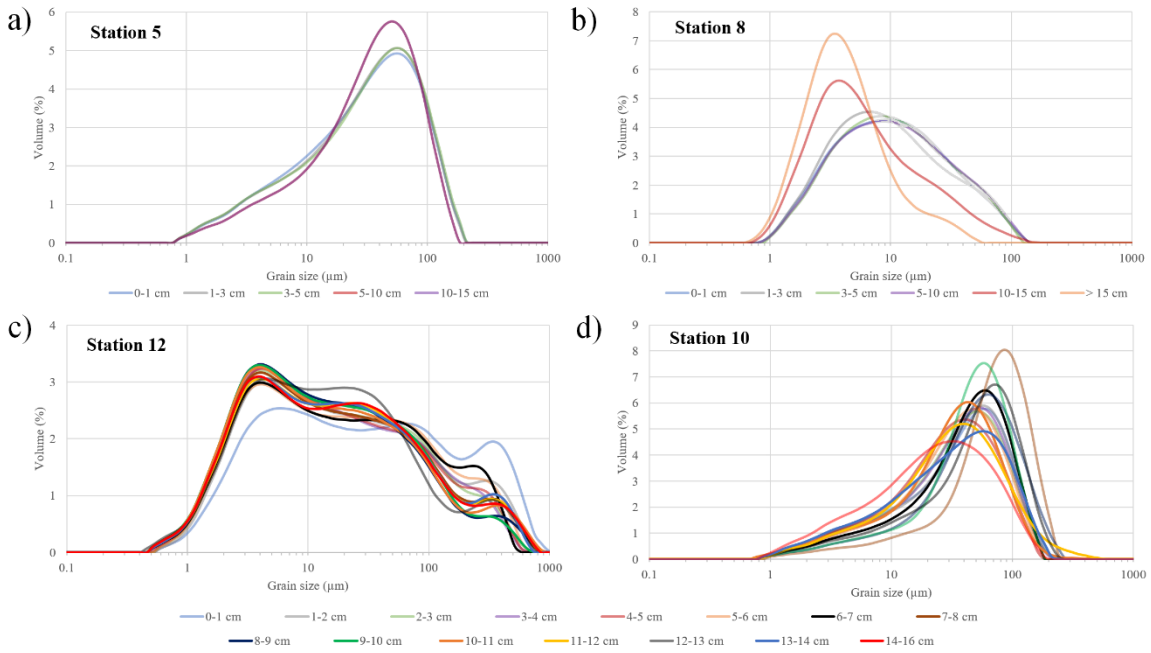

Figure S5. Grain size distribution in volume of seafloor sediments at stations **(a)** 5, **(b)** 8, **(c)** 12 and **(d)** 10. Each curve represents a slice of sediment.

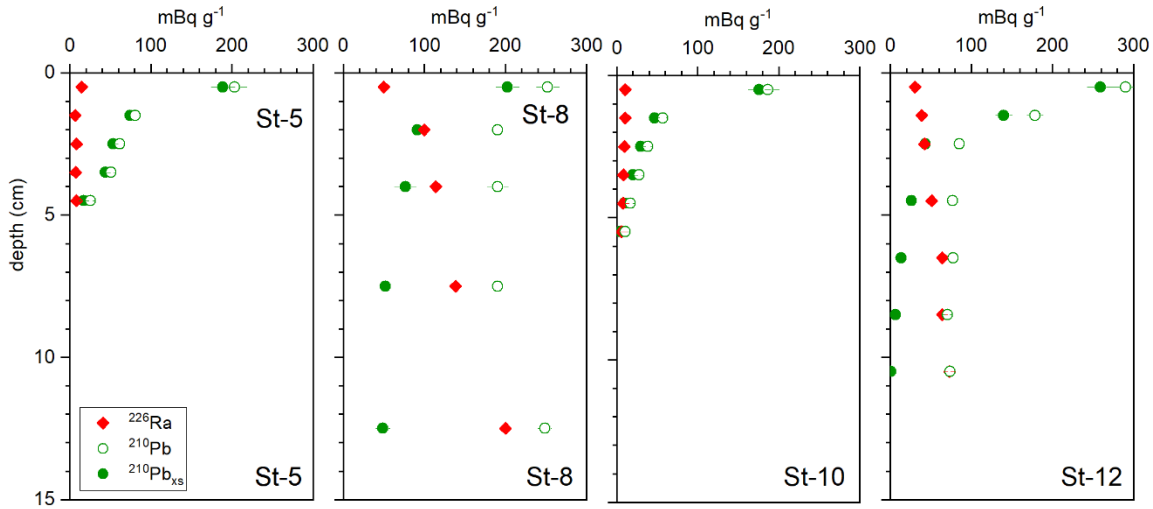

Figure S6. Depth profiles of ^{226}Ra, ^{210}Pb and $^{210}Pb_{XS}$ activities

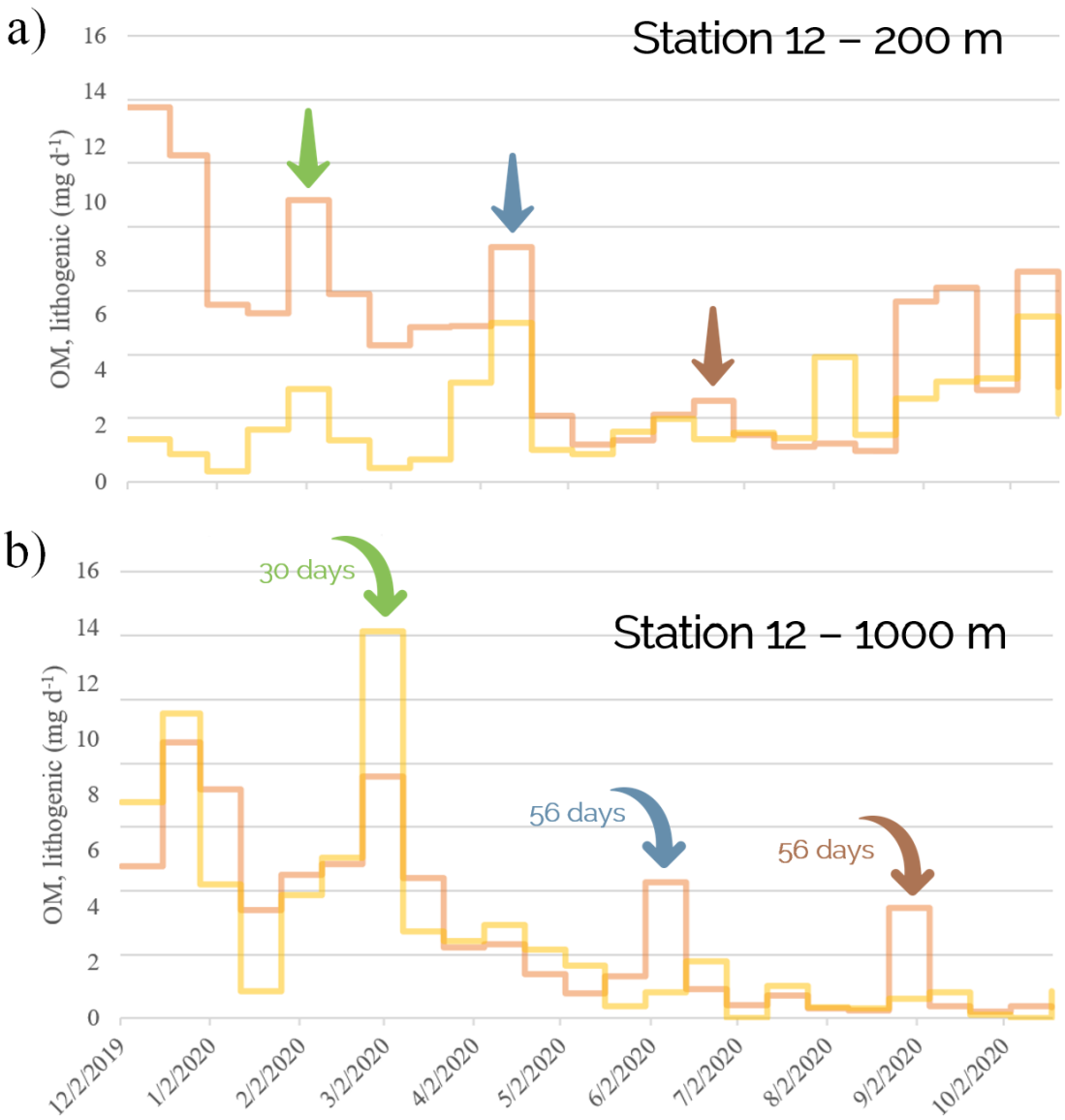

Figure S7. Temporal dynamics of exported material (mg d^{-1}) in the fixed sediment trap at **(a)** 200 and **(b)** 1000 m: organic matter (orange line) and lithogenic fraction (yellow line). The arrows indicate the collection time lag of the material peaks concerned. Each distinct color illustrates the time lag between the peak of material initially collected at 200 m and the peak subsequently collected at 1000 m for particles originating from the Tonga Arc.

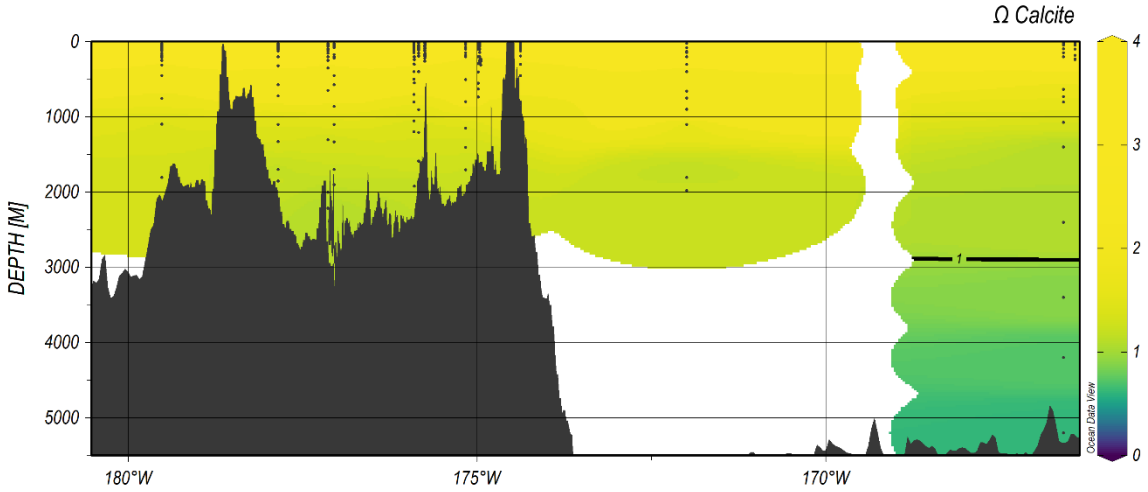

Figure S8. Calcite saturation rates on the cruise transect. Rates were calculated from pH and total alkalinity data (see *Texts S3-S4* for protocols) via the *seacarb* package of R software (Lavigne and Gattuso, 2010). Note that the lysocline is represented by an $\Omega_{calcite}$ equal to 1. Below this layer ($\Omega < 1$), the rate of calcite dissolution will increase dramatically (Woosley, 2018). Not far from the lysocline is the carbonate compensation depth, below which no carbonate is preserved within the seafloor sediments (Holmén, 2000).

Table S1. Percentage recovery of GBW certified reference material, blanks and limits of detection and quantification (in ppm) for each element analyzed by ICP-OES.

	Fe	Al	Ca	Mn	Cu	Zn	Cr	Pb	Ni
GBW percent recovery	104	101	100	102	113	103	111	80	105
Blanks	< DL	< DL	12 ± 1	15 ± 1	3.5 ± 1.9	1.6 ± 0.6	0.8 ± 0.6	2.6 ± 0.7	< DL
Detection limit	0.3	0.8	*n.d.*	0.2	1	0.5	0.7	*n.d.*	1.3
Quantification limit	0.6	2.7	*n.d.*	0.3	1.9	1.1	1.6	*n.d.*	3.5

Note. GBW is a marine reference sediment provided by the National Research Council for Certified Reference Materials (Canada). ICP-OES stands for Inductively-Coupled Plasma Optical Emission Spectrometry.

Table S2. Estimated calcium carbonate fraction in sinking material and seafloor sediment from %PIC or %Ca

Sample	Collecting day	Sampling period	$CaCO_3$ from PIC	$CaCO_3$ from Ca
		day	*%*	*%*
TD-ST5 1000-1	11/10/2019	1.0	40.1	43.0
TD-ST5 1000-2	11/11/2019	1.0	71.7	65.0
TD-ST5 1000-3	11/12/2019	1.0	73.6	66.0
TD-ST5 1000-4	11/13/2019	1.0	52.4	50.8
TD-ST5 1000-5	11/14/2019	1.0	44.8	43.1
TD-ST10 1000-1	11/24/2019	1.0	14.9	19.7
TD-ST10 1000-2	11/25/2019	1.0	9.6	14.2
TD-ST10 1000-3	11/26/2019	1.0	13.2	16.2
TD-ST10 1000-4	11/27/2019	1.0	14.3	18.6
TD-ST10 200-1	11/24/2019	1.0	n.d.	44.4
TD-ST10 200-2	11/25/2019	1.0	n.d.	55.6
TD-ST10 200-3	11/26/2019	1.0	n.d.	65.4
TD-ST10 200-4	11/27/2019	1.0	n.d.	49.2
TF-200-01	12/2/2019	14.0	61.4	49.1
TF-200-02	12/16/2019	14.0	52.5	47.6
TF-200-03	12/29/2019	14.0	63.6	57.1
TF-200-04	1/12/2020	14.0	46.0	50.1
TF-200-05	1/26/2020	14.0	23.3	40.3
TF-200-06	2/9/2020	14.0	4.6	47.7
TF-200-07	2/23/2020	14.0	69.5	49.5
TF-200-08	3/8/2020	14.0	81.8	35.8
TF-200-09	3/22/2020	14.0	44.5	54.7

TF-200-10	4/5/2020	14.0	28.8	48.2
TF-200-11	4/19/2020	14.0	41.0	68.1
TF-200-12	5/3/2020	14.0	38.4	60.3
TF-200-13	5/17/2020	14.0	53.8	63.6
TF-200-14	5/31/2020	14.0	52.3	66.3
TF-200-15	6/14/2020	14.0	35.8	63.9
TF-200-16	6/28/2020	14.0	63.7	100.4
TF-200-17	7/12/2020	14.0	40.7	81.4
TF-200-18	7/26/2020	14.0	62.7	53.2
TF-200-19	8/9/2020	14.0	49.9	60.4
TF-200-20	8/23/2020	14.0	52.6	56.1
TF-200-21	9/6/2020	14.0	23.9	66.9
TF-200-22	9/20/2020	14.0	61.5	67.2
TF-200-23	10/4/2020	14.0	25.4	50.3
TF-200-24	10/18/2020	14.0	17.6	60.3
TF-1000-01	12/2/2019	14.0	56.8	63.1
TF-1000-02	12/16/2019	14.0	59.4	56.3
TF-1000-03	12/29/2019	14.0	60.9	56.6
TF-1000-04	1/12/2020	14.0	69.3	62.4
TF-1000-05	1/26/2020	14.0	53.0	59.5
TF-1000-06	2/9/2020	14.0	54.8	61.1
TF-1000-07	2/23/2020	14.0	51.9	65.6
TF-1000-08	3/8/2020	14.0	60.1	58.5
TF-1000-09	3/22/2020	14.0	57.4	75.1
TF-1000-10	4/5/2020	14.0	64.1	68.2
TF-1000-11	4/19/2020	14.0	60.9	38.5
TF-1000-12	5/3/2020	14.0	65.3	67.2
TF-1000-13	5/17/2020	14.0	77.8	54.1
TF-1000-14	5/31/2020	14.0	12.0	26.0
TF-1000-15	6/14/2020	14.0	58.4	67.9
TF-1000-16	6/28/2020	14.0	59.6	143.4
TF-1000-17	7/12/2020	14.0	49.3	94.4
TF-1000-18	7/26/2020	14.0	61.9	59.2
TF-1000-19	8/9/2020	14.0	71.8	75.0
TF-1000-20	8/23/2020	14.0	14.1	47.2
TF-1000-21	9/6/2020	14.0	38.3	194.1
TF-1000-22	9/20/2020	14.0	72.4	139.3
TF-1000-23	10/4/2020	14.0	93.2	33.3
TF-1000-24	10/18/2020	14.0	69.1	85.0
SC-ST5 00-01 cm	-	-	2.1	13.3
SC-ST5 01-03 cm	-	-	0.9	12.7
SC-ST5 03-05 cm	-	-	1.0	15.2

SC-ST5 05-10 cm	-	-	1.0	15.5
SC-ST5 10-15 cm	-	-	3.9	18.7
	-	-	0.0	0.0
SC-ST10 00-01 cm	-	-	8.0	22.4
SC-ST10 01-02 cm	-	-	6.3	19.7
SC-ST10 02-03 cm	-	-	5.1	18.9
SC-ST10 03-04 cm	-	-	4.6	18.8
SC-ST10 04-05 cm	-	-	0.8	12.7
SC-ST10 05-06 cm	-	-	3.8	18.1
SC-ST10 06-07 cm	-	-	2.9	17.8
SC-ST10 07-08 cm	-	-	1.4	16.7
SC-ST10 08-09 cm	-	-	2.9	17.6
SC-ST10 09-10 cm	-	-	3.9	18.6
SC-ST10 10-11 cm	-	-	4.4	18.0
SC-ST10 11-12 cm	-	-	3.0	16.1
SC-ST10 12-13 cm	-	-	2.6	18.1
SC-ST10 13-14 cm	-	-	3.7	16.5
SC-ST10 14-16 cm	-	-	3.4	15.4
	-	-		
SC-ST12 00-01 cm	-	-	64.0	69.6
SC-ST12 01-02 cm	-	-	62.0	70.9
SC-ST12 02-03 cm	-	-	62.9	67.5
SC-ST12 03-04 cm	-	-	64.0	64.7
SC-ST12 04-05 cm	-	-	64.8	75.1
SC-ST12 05-06 cm	-	-	64.9	64.2
SC-ST12 06-07 cm	-	-	66.1	67.8
SC-ST12 07-08 cm	-	-	65.4	70.5
SC-ST12 08-09 cm	-	-	64.2	67.1
SC-ST12 09-10 cm	-	-	65.2	68.6
SC-ST12 10-11 cm	-	-	64.4	69.1
SC-ST12 11-12 cm	-	-	64.9	72.9
SC-ST12 12-13 cm	-	-	64.0	67.9
SC-ST12 13-14 cm	-	-	62.8	64.3
SC-ST12 14-15 cm	-	-	63.0	66.3
	-	-		
SC-ST8 00-01 cm	-	-	0.4	6.3
SC-ST8 01-03 cm	-	-	0.2	7.2
SC-ST8 03-05 cm	-	-	0.2	7.1
SC-ST8 05-10 cm	-	-	0.2	6.8
SC-ST8 10-15 cm	-	-	0.2	4.6
SC-ST8 >>15 cm	-	-	0.4	3.3

Note. The calcium carbonate fraction can be estimated from %PIC (%CaCO3 = %PIC × 8.33) or %Ca (%CaCO3 = 0.4 × %Ca). The calcium carbonate fraction of some samples was overestimated (> 100% of total collection weight) with the %Ca method. TD refers to drifting traps. TF refers to

fixed trap (Station 12 only). SC refers to sediment cores. PIC stands for particulate inorganic carbon.

Table S3. Highlights of the productivity measured at the stations studied during the TONGA cruise (austral summer conditions).

Sample	Station 5	Station 8	Station 10	Station 12
Primary productivity	90	< 35	145	n.d.
N_2 fixation	2727	225	1803	n.d.
Max total Chl-*a*	0.45	0.22	0.38	0.33
Cyanobacteria	70.3 ± 4.4	65.1 ± 7.5	68.6 ± 4.5	65.3 ± 4.6
Coccolithophores	22.9 ± 5.1	22.2 ± 3.6	24.8 ± 3.8	25.4 ± 4.0
Dinoflagellates, diatoms	6.7 ± 3.9	12.7 ± 7.9	6.5 ± 3.3	9.1 ± 4.3

Note. Primary production is in mmol C m^{-2} d^{-1}, dinitrogen (N_2) fixation is in µmol N m^{-2} d^{-1}. Maximum total chlorophyll-*a* (Chl-*a*) is in mg m^{-3}. The major groups contributing to total Chl-*a* are represented in %. Photosynthetic pigment data were obtained by high-performance liquid chromatography (Van Heukelem and Thomas, 2001). The contribution of cyanobacteria, coccolithophores, dinoflagellates and diatoms to total Chl-*a* was estimated from zeaxanthin, 19'-hexanoyloxyfucoxanthin, peridinin and fucoxanthin, respectively, following Uitz et al. (2006). The data presented in this table will be accessible as soon as they are published on the LEFE-CYBER database (http://www.obs-vlfr.fr/proof/php/TONGA/tonga.php).

Table S4. Boström index values in each cup of the traps and in each sediment slice.

Station	Date/slice	Depth	Fe_{cfb}	Al_{cfb}	Mn_{cfb}	Boström index
-	*-/cm*	*m*		*wt.%*		-
Station 5	11/10/2019	1000-01	0.97	1.01	0.03	50.31
	11/11/2019	1000-02	1.99	2.15	0.05	51.24
	11/12/2019	1000-03	2.44	2.60	0.07	50.87
	11/13/2019	1000-04	0.92	0.96	0.03	50.49
	11/14/2019	1000-05	0.80	0.83	0.03	50.01
	00-01 cm	Seafloor	7.52	6.11	2.78	37.22
	01-03 cm	Seafloor	7.65	6.05	2.09	38.33
	03-05 cm	Seafloor	8.66	7.38	2.58	39.64
	05-10 cm	Seafloor	8.48	7.05	2.35	39.44
	10-15 cm	Seafloor	7.81	7.34	1.54	43.96
Station 10	11/24/2019	200-01	0.47	0.22	0.08	28.61
	11/25/2019	200-02	0.55	0.09	0.10	11.64
	11/26/2019	200-03	0.37	0.17	0.12	26.28
	11/27/2019	200-04	0.28	0.15	0.09	28.66
	11/24/2019	1000-01	3.03	5.88	0.01	65.92
	11/25/2019	1000-02	2.99	6.17	0.01	67.35
	11/26/2019	1000-03	2.87	5.81	0.00	66.93
	11/27/2019	1000-04	2.93	5.79	0.01	66.34
	00-01 cm	Seafloor	7.48	7.38	1.78	44.37
	01-02 cm	Seafloor	7.69	7.50	1.65	44.54
	02-03 cm	Seafloor	7.84	7.63	1.69	44.47
	03-04 cm	Seafloor	7.67	7.30	1.58	44.11
	04-05 cm	Seafloor	7.51	6.28	1.46	41.19
	05-06 cm	Seafloor	8.07	7.53	1.54	43.95
	06-07 cm	Seafloor	8.02	7.67	1.49	44.64
	07-08 cm	Seafloor	7.90	7.58	1.36	45.01
	08-09 cm	Seafloor	7.83	7.65	1.43	45.21
	09-10 cm	Seafloor	7.66	7.52	1.49	45.10
	10-11 cm	Seafloor	7.41	7.53	1.46	45.90
	11-12 cm	Seafloor	6.80	7.18	1.23	47.20
	12-13 cm	Seafloor	7.71	7.80	1.49	45.87
	13-14 cm	Seafloor	6.59	7.30	1.50	47.42
	14-16 cm	Seafloor	6.27	7.40	1.29	49.46
Station 12	12/2/2019	200-01	0.13	0.12	0.006	47.00
	12/16/2019	200-02	0.04	0.02	0.003	34.90
	12/29/2019	200-03	0.73	1.03	0.003	58.39
	1/12/2020	200-04	0.99	1.70	0.003	63.18
	1/26/2020	200-05	0.53	1.02	0.002	65.76
	2/9/2020	200-06	0.69	0.97	0.002	58.25
	2/23/2020	200-07	0.75	0.66	0.003	46.83
	3/8/2020	200-08	2.07	2.44	0.006	54.10
	3/22/2020	200-09	1.73	2.94	0.007	62.86
	4/5/2020	200-10	1.35	2.77	0.006	67.13
	4/19/2020	200-11	1.02	2.42	0.007	70.07
	5/3/2020	200-12	0.89	1.83	0.006	67.15
	5/17/2020	200-13	1.83	3.38	0.008	64.74
	5/31/2020	200-14	2.46	3.10	0.011	55.63
	6/14/2020	200-15	3.64	7.33	0.008	66.80
	6/28/2020	200-16	1.84	0.32	0.003	14.73
	7/12/2020	200-17	1.04	1.50	0.004	58.95
	7/26/2020	200-18	0.20	0.06	0.001	21.44
	8/9/2020	200-19	1.34	2.39	0.003	64.01
	8/23/2020	200-20	0.92	1.21	0.003	56.78
	9/6/2020	200-21	1.68	2.36	0.007	58.26
	9/20/2020	200-22	1.80	2.15	0.004	54.43
	10/4/2020	200-23	1.45	3.09	0.002	68.09
	10/18/2020	200-24	0.91	1.17	0.005	55.89
	12/2/2019	1000-01	0.94	0.63	0.05	38.93
	12/16/2019	1000-02	2.88	3.08	0.10	50.74
	12/29/2019	1000-03	1.49	1.37	0.07	46.72

	1/12/2020	1000-04	1.44	1.64	0.03	52.68
	1/26/2020	1000-05	0.53	0.26	0.05	31.07
	2/9/2020	1000-06	0.75	0.54	0.06	39.96
	2/23/2020	1000-07	0.77	0.34	0.06	29.36
	3/8/2020	1000-08	1.27	1.11	0.09	44.93
	3/22/2020	1000-09	0.91	0.61	0.08	38.22
	4/5/2020	1000-10	0.71	0.46	0.06	37.42
	4/19/2020	1000-11	0.49	0.34	0.04	39.02
	5/3/2020	1000-12	0.28	0.15	0.03	32.88
	5/17/2020	1000-13	0.52	0.45	0.05	43.85
	5/31/2020	1000-14	0.05	0.05	0.01	48.61
	6/14/2020	1000-15	0.35	0.14	0.03	26.98
	6/28/2020	1000-16	0.25	0.25	0.02	48.04
	7/12/2020	1000-17	0.27	0.34	0.02	53.71
	7/26/2020	1000-18	0.33	0.31	0.03	46.07
	8/9/2020	1000-19	0.69	0.62	0.05	45.65
	8/23/2020	1000-20	0.04	0.04	0.00	50.44
	9/6/2020	1000-21	0.18	0.17	0.01	47.50
	9/20/2020	1000-22	0.50	0.45	0.04	45.70
	10/4/2020	1000-23	2.85	2.53	0.20	45.33
	10/18/2020	1000-24	0.63	0.46	0.04	40.57
	00-01 cm	Seafloor	5.75	4.17	13.83	17.56
	01-02 cm	Seafloor	6.09	4.47	15.16	17.37
	02-03 cm	Seafloor	6.77	4.92	17.49	16.87
	03-04 cm	Seafloor	7.71	5.70	20.26	16.92
	04-05 cm	Seafloor	6.82	4.67	17.82	15.92
	05-06 cm	Seafloor	6.66	4.83	17.30	16.77
	06-07 cm	Seafloor	6.88	5.00	19.38	16.00
	07-08 cm	Seafloor	6.98	5.05	20.13	15.69
	08-09 cm	Seafloor	6.83	5.13	20.00	16.05
	09-10 cm	Seafloor	6.96	4.92	19.87	15.49
	10-11 cm	Seafloor	6.76	4.80	19.88	15.26
	11-12 cm	Seafloor	7.14	4.65	18.40	15.39
	12-13 cm	Seafloor	6.88	4.81	19.27	15.54
	13-14 cm	Seafloor	3.51	2.35	9.75	13.41
	14-15 cm	Seafloor	3.66	3.61	18.33	14.10
Station 8	00-01 cm	Seafloor	6.12	6.63	5.59	36.16
	01-03 cm	Seafloor	6.69	7.15	4.99	37.98
	03-05 cm	Seafloor	6.45	7.05	4.55	39.06
	05-10 cm	Seafloor	6.44	6.99	4.34	39.35
	10-15 cm	Seafloor	6.13	7.33	6.15	37.37
	>>15 cm	Seafloor	5.64	7.08	6.45	36.93

Note. The concentrations in calcium-carbonate-free basis (*cfb*) of the elements used for the calculation of the index (Al_{cfb}, Fe_{cfb}, Mn_{cfb}) are also represented.